Study of the f(0)(1500)/f(2)(1565) production in the exclusive annihilation anti-n.anti-p -> pi+.pi+.pi- in flight

Study of the $f_0(1500)/f_2(1565)$ production in the exclusive annihilation $\bar{n}p \to \pi^+\pi^+\pi^-$ in flight

A. Bertin, M. Bruschi, M. Capponi, A. Collamati, S. De Castro, R. Donà, A. Ferretti, D. Galli, B. Giacobbe, U. Marconi, M. Piccinini, M. Poli,* N. Semprini Cesari, R. Spighi, S. Vecchi, A. Vezzani, F. Vigotti, M. Villa, A. Vitale, and A. Zoccoli
Dipartimento di Fisica, Università di Bologna and INFN, Sezione di Bologna, Bologna, Italy

M. Corradini, A. Donzella, E. Lodi Rizzini, L. Venturelli, and A. Zenoni
Dipartimento di Chimica e Fisica per l'Ingegneria e per i Materiali, Università di Brescia and INFN, Sezione di Pavia, Pavia, Italy

C. Cicalò, A. Masoni, G. Puddu, S. Serci, P. Temnikov,† and G. Usai
Dipartimento di Fisica, Università di Cagliari and INFN, Sezione di Cagliari, Cagliari, Italy

O. E. Gortchakov, S. N. Prakhov, A. M. Rozhdestvensky, M. G. Sapozhnikov, and V. I. Tretyak
Joint Institute for Nuclear Research, Dubna, Moscow, Russia

P. Gianotti, C. Guaraldo, A. Lanaro, V. Lucherini, F. Nichitiu,‡ C. Petrascu,‡ and A. Rosca‡
Laboratori Nazionali di Frascati dell'INFN, Frascati, Italy

V. Ableev,§ C. Cavion, U. Gastaldi, M. Lombardi, G. Maron, L. Vannucci, and G. Vedovato
Laboratori Nazionali di Legnaro dell'INFN, Legnaro, Italy

G. Bendiscioli, V. Filippini, A. Fontana, P. Montagna, A. Rotondi, A. Saino, P. Salvini, and C. Scoglio
Dipartimento di Fisica Nucleare e Teorica, Università di Pavia and INFN, Sezione di Pavia, Pavia, Italy

F. Balestra, D. Bergo, E. Botta, T. Bressani, M. P. Bussa, L. Busso, D. Calvo, P. Cerello, S. Costa, P. Damiani, O. Y. Denisov,§ F. D'Isep, C. Fanara, L. Fava, A. Feliciello, L. Ferrero, A. Filippi,‖ R. Garfagnini, A. Grasso, A. Maggiora, S. Marcello, N. Mirfakhrai,¶ D. Panzieri, E. Rossetto, F. Tosello, and L. Valacca
Istituto di Fisica, Università di Torino and INFN, Sezione di Torino, Torino, Italy

M. Agnello, F. Iazzi, and B. Minetti
Politecnico di Torino, Dipartimento di Fisica and INFN, Sezione di Torino, Torino, Italy

G. Pauli and S. Tessaro
Istituto di Fisica, Università di Trieste and INFN, Sezione di Trieste, Trieste, Italy

L. Santi
Istituto di Fisica, Università di Udine and INFN, Sezione di Trieste, Italy

(The OBELIX Collaboration)

(Received 19 May 1997; revised manuscript received 20 August 1997; published 9 December 1997)

The spin-parity analysis of the $\bar{n}p \to \pi^+\pi^+\pi^-$ exclusive reaction in flight is presented. The main aim is to study the $(\pi^+\pi^-)$ invariant mass spectrum in the region around 1500 MeV. The analysis was performed with a Breit-Wigner parametrization for all the resonant states and, for the scalar sector in the mass region below 1.2 GeV, by means of a K-matrix-like treatment. It clearly shows the need for two states, a scalar one (0^{++}) with mass and width (1522 ± 25) MeV and (108 ± 33) MeV, and a tensorial one (2^{++}) with mass (1575 ± 18) MeV and width (119 ± 24) MeV, respectively. In addition, the analysis requires the presence of a scalar state at (1280 ± 55) MeV, (323 ± 13) MeV broad, and of a second vectorial one, in addition to the $\rho^0(770)$ signal, with mass and width (1348 ± 33) MeV and (275 ± 10) MeV, respectively. [S0556-2821(98)01401-5]

PACS number(s): 13.75.Cs, 12.39.Mk, 14.40.Cs

*Dipartimento di Energetica ''Sergio Stecco,'' Università di Firenze, Firenze, Italy.

†On leave of absence from Institute for Nuclear Research and Nuclear Energy, Sofia, Bulgaria.

‡On leave of absence from National Institute of Research and Development for Physics and Nuclear Engineering ''Horia Hulubei,'' Bucharest-Magurele, Romania.

§On leave of absence from Joint Institute for Nuclear Research, Dubna, Moscow, Russia.

‖Corresponding author. E-mail address: filippi@to.infn.it; FAX: ++.39.11.6707325

¶On leave of absence from Shahid Beheshty University, Teheran, Iran.

I. INTRODUCTION

The annihilation of a $(\mathcal{N}\overline{\mathcal{N}})$ system provides a useful tool to study the production of new mesons, in addition to the ordinary $q\overline{q}$-like ones which find a natural location in the SU(3) nonets. In fact, it helps us to understand whether new objects, which are unlikely to be classified as ordinary mesons due both to their quantum numbers and to the lack of available slots in the nonets, are due to effects related to $(\mathcal{N}\overline{\mathcal{N}})$ dynamics or are items of a new kind of matter, composed by gluons only (the glueballs) or by mixings between quarks and gluons. The existence of such non-$q\overline{q}$ mesons is predicted by QCD, which up to now is the most reliable theory for the description of strong interaction phenomena, but still has to be fully proved on experimental grounds.

A possible candidate for a glueball state is a relatively ''new'' resonant structure emerging at about 1500 MeV in the $(\pi^+\pi^-)$ invariant mass spectra, observed in the final states of $\mathcal{N}\overline{\mathcal{N}}$ annihilation reactions.

After the initial observation of a state at about 1500 MeV in annihilation processes in liquid hydrogen and deuterium bubble chambers [1], its first sound spin-parity assignment was given by the Asterix Collaboration by means of a comparative study of the $\overline{p}p\to\pi^+\pi^-\pi^0$ annihilation reaction at rest, in two separate samples, experimentally selected and characterized by a different content of P-wave initial states [2]. Its observation, mainly in the P-wave enriched sample, and a complete spin-parity analysis by means of Breit-Wigner parametrization for resonances, led them to assert its tensorial (2^{++}) nature. The mass and width were found to be 1565 ± 20 MeV and 170 ± 40 MeV, respectively; this state is reported in the last Particle Data Group (PDG) issue [3] as $f_2(1565)$.

The study of the $\overline{p}p\to\pi^+\pi^-\pi^0$ channel is rather difficult; complications arise from the double isospin choice for the $p\overline{p}$ state ($I=0$ or $I=1$) and from the presence of several intermediate states, such as the ρ's triplet, which interfere in the $\pi\pi$ mass region around 1500 MeV. The Asterix and the OBELIX experiments could overcome these complications by exploiting different techniques allowing a reliable selection of the initial state (i.e., the simultaneous detection of L-X rays [2] and the use of targets in different pressure conditions [4]). On the other hand, when studying the $p\overline{p}\to 3\pi^0$ annihilation channel, one has to deal with combinatorial effects, but in this case the isospin is fixed (to 1), so that the total number of initial states is reduced by I and J^{PC} conservation laws. The Crystal Barrel Collaboration extensively studied this channel and published several papers about the properties of the state at about 1500 MeV, each time with increased statistics and with improved analysis methods [5–9]: The first paper asserted the presence of a tensorial resonance, at $m=1515$ MeV, which could really be identified with the 2^{++} state found by Asterix [5]. Later on the need for a scalar signal was put forward [6,10]. A scalar component was then added to a tensorial one, of reduced strength, to obtain good fits [7]; this scalar state is now classified as $f_0(1500)$ [3]. These results were confirmed by an updated study with high statistics (712 000 events) [8]. The new study was performed by applying the K-matrix analysis technique [11], which assures unitarity even in the presence of several overlapping states with the same quantum numbers. It led to the conclusion that, in addition to the narrow $f_0(975)$ and a broad $f_0(1300)$ backgroundlike signal reported now by PDG [3] as $f_0(1370)$, a third scalar resonance of mass (1500 ± 15) MeV and width $\Gamma=(120\pm 25)$ MeV is actually needed, as well as a second D-wave contribution [in addition to $f_2(1270)$], at about 1520 MeV. The fractional contribution of these two states to the $3\pi^0$ annihilation channel was found to be 12% for the $f_0(1500)$ and 17% for the $f_2(1520)$. These results were recently confirmed by a coupled-channel analysis [9] on $\overline{p}p\to 3\pi^0$, $\overline{p}p\to 2\eta\pi^0$, and $\overline{p}p\to 2\pi^0\eta$ data samples, and the mass for the tensorial signal was suggested to be about 1552 MeV.

A number of results by OBELIX concerning the properties of the structures at about 1500 MeV have been published [12–14]. They show that a single tensorial signal is by no means enough to give a good description of the structure at about 1500 MeV. An attempt to introduce a scalar contribution was quite successful, and it was shown that it could be dominant especially below 1550 MeV. On the contrary, for higher masses a contribution from a tensorial state seemed to be required by the fit.

In this paper we report the results of the study of the $f_0(1500)/f_2(1565)$ resonances in the in-flight annihilation reaction $\overline{n}p\to 2\pi^+\pi^-$, taking into account a possible dependence on the $\overline{n}$ momentum as well.

II. $\overline{n}p\to\pi^+\pi^+\pi^-$ REACTION

A. Experimental environment

Concerning the selection of $\mathbf{I}=\mathbf{1}$ initial states, the same properties of the $p\overline{p}\to 3\pi^0$ annihilation channel are shared by other reactions, such as $\overline{p}d\to 2\pi^-\pi^+p_s$ and $\overline{n}p\to 2\pi^+\pi^-$. While the first was initially studied in bubble chamber [1,15], the second one could never be investigated due to the lack of $\overline{n}$ beams. Only the OBELIX experiment could study such annihilations thanks to a unique facility which allowed the production of antineutrons by means of a $\overline{p}p\to n\overline{n}$ charge exchange reaction [16].

1. Experimental apparatus and the production of the $\overline{n}$ beam

Only a few hints will be given here about the experimental setup and its main performances; a more detailed description may be found, for example, in Ref. [17].

OBELIX is a magnetic spectrometer which operated at the CERN LEAR machine until its closure. It was designed in order to study low energy antiprotons and antineutrons annihilations on nucleons and nuclei, with the main purpose of investigating nuclear dynamics effects and meson spectroscopy with high statistics. The apparatus exhibits a cylindrical symmetry and its central detectors operate in a 0.5 T magnetic field provided by the Open Axial Field magnet. Moving radially from the axis, coincident with the $\overline{p}/n$ beam line, it is composed of the following: a cylindrical target, filled with different gases or liquids according to the measurement to be performed; a spiral projection chamber as vertex detector; two cylindrical layers of plastic scintillators,

TABLE I. Total three-prong statistics under study: real data and Monte Carlo–generated events. In the text we refer, for simplicity of notation, to each of the data samples by the numbers 1, 2, 3, and 4 for the global one.

	$p_{\bar{n}}$ range	Experimental events	Monte Carlo events
1	$\sim 50 \leqslant p_{\bar{n}} \leqslant 200$ MeV/c	5468	15000
2	$200 < p_{\bar{n}} \leqslant 300$ MeV/c	16666	74000
3	$300 < p_{\bar{n}} \leqslant 405$ MeV/c	18347	70000
4	global: $\sim 50 \leqslant p_{\bar{n}} \leqslant 405$ MeV/c	35118	90000

which constitute the time-of-flight (TOF) system and which sandwich the tracking device, a Jet Drift Chamber. The time-of-flight system provides in real time ($\sim$200 ns) information about the multiplicity of the annihilation event and its topology and delivers a fast signal on which the first level trigger of the apparatus is based [18]. It allows charged particle (K, p, π) identification, at least up to 600 MeV/c momenta, and moreover it is essential for the evaluation of the $\bar{n}$ momentum; its overall resolution is about 1 ns full width at half maximum (FWHM). The tracking device is also used for particle identification by dE/dx measurements. Its spatial resolution is about $\sigma_{\rho\phi}=160$ μm in the ($\rho\phi$) plane and $\sigma_z=1.2$ cm along the wires; dE/dx resolution is about $\sigma_E/E \sim 12\%$ and allows one to discriminate pions from kaons up to 600 MeV/c, and to identify protons up to 1 GeV/c. Its momentum resolution is $\sim$3.2% at 930 MeV/c. Finally, four supermodules of a High Angular Resolution Gamma Detector enclose the central detector.

The apparatus is endowed with a facility, unique in the world, for the production of an antineutron beam. The antineutron production occurs in a LH_2 cylindrical target placed along the $\bar{p}$-beam axis in the upstream hollow pole of the magnet, at about 2 m from the center of the apparatus; its length depends on the momentum of the incoming antiprotons [19].

The produced antineutrons are collimated by a suitable lead collimator system and then annihilate in the reaction target placed at the center of the apparatus (instead of the vertex detector); depending on the $\bar{p}$ beam momentum and on the collimator shape, the number of produced $\bar{n}$'s lies in the range 30–50/10^6 $\bar{p}$, and out of these about 20% interact in flight in the reaction target. The features of the $\bar{n}$ beam are continuously kept under control by a suitable monitor placed downstream the spectrometer.

The measurement of each $\bar{n}$ momentum is performed by means of the time-of-flight technique, measuring the time between the arrival of an antiproton and the impact time of the fastest of the annihilation products on the inner scintillator barrel system. This measurement is affected by a total error less than 5% [19]. The $\bar{n}$'s are produced with a continuous momentum distribution ranging from $\sim$50 MeV/c ($\bar{n}$ from $\bar{p}$ with 98.6 MeV/c, the CEX threshold momentum) up to a maximum depending on the $\bar{p}$ momentum, and corresponding in general to $\bar{n}$ production near the entrance window of the target.

The full description of this facility and its performances may be found in Ref. [19].

2. Meson spectroscopy with $\bar{n}$

Even if the globally available statistics is lower than what could be obtained in the $\bar{p}d$ reaction, and the experimental realization of the $\bar{n}$ beam a rather difficult challenge, the $\bar{n}p$ annihilation has the advantage that the final states are completely unaffected by the rescattering problems which, on the contrary, spoil the observations of $\bar{p}n$ ones. As will be shown later, $\bar{n}p \to 2\pi^+\pi^-$ events can be selected by means of a 4C kinematic fit which rejects most of the background contribution. Moreover, they do not suffer combinatorial effects as strong as those emerging, for example, in the $3\pi^0$ channel.

Since the antineutrons annihilate in flight, the available energy for the annihilation reaction changes event by event. This lets studying various annihilation effects, such as the production rates of initial partial waves and the branching fractions of intermediate states, as a function of $\bar{n}$ momentum. However, care must be taken when dealing with amplitudes as well as with normalizations, since both of them vary event by event as a function of the available energy. Moreover, the amplitude should take into account that in in-flight annihilation it is necessary to sum incoherently over polarizations [20,21].

B. Data reduction criteria

With the $\bar{n}$ facility a total of about 21×10^6 annihilations in a liquid hydrogen target have been collected, in different LEAR beam conditions ($p_{\bar{p}} \simeq 305$ MeV/c in 1991–1992, $p_{\bar{p}} \simeq 412$ MeV/c in 1993–1994–1995, entailing different maxima for $\bar{n}$ momentum). In Table I the total available statistics for three-prong events is reported, selected according to four $p_{\bar{n}}$ intervals.

The analysis has been performed independently on all of the reported $p_{\bar{n}}$ different ranges. Each sample had to be matched with a dedicated Monte Carlo calculation, whose event content is reported in Table I as well. The Monte Carlo–generated events have been reduced applying the same selection criteria as for the experimental data; it was chosen not to mix more than two samples belonging to different data taking periods, for consistency reasons.

Useful data are selected applying powerful quality cuts which drastically reduce the total background. All events have been collected by applying a loose multiplicity trigger (by means of OBELIX time-of-flight system: the tighter requirement was of at least three and two hits, respectively, on the inner and outer detectors); the off-line analysis discarded events either not fully reconstructed in the OBELIX tracking

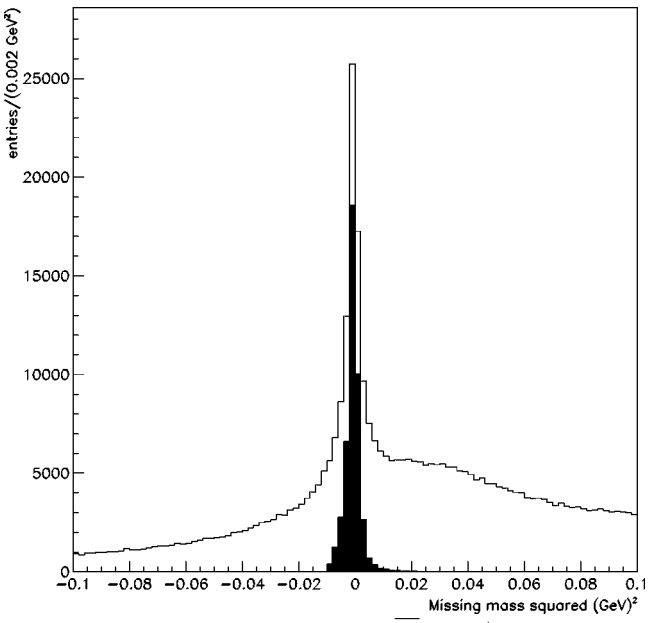

FIG. 1. Missing mass spectrum for $\overline{n}p \to 2\pi^+\pi^-$ events with topological selection only (white area) and for events selected by applying energy-momentum conservation cuts and 4C kinematic fit (black area).

device and not showing a common vertex or with a wrong total charge and multiplicity, as well as annihilations occurring outside the reaction target or on its mylar walls. Energy-momentum conservation cuts were employed so as to eliminate possible undetected neutral particles; the total energy was required to be larger than 1.8 GeV and the total c.m. momentum less than 100 MeV/c. All surviving events were then submitted to a 4C kinematic fit to check the $\overline{n}p \to 2\pi^+\pi^-$ hypothesis, and out of it only those with a confidence level larger than 5% have been selected; a further rejection was applied to events whose confidence level, for the 1C fit to the kinematic hypothesis $\overline{n}p \to 2\pi^+\pi^-\pi^0$, turned out to be larger than 5% too. At the end of data selection the background contribution was reduced to 0.4% of the globally available statistics. In Fig. 1 the missing mass spectrum for the events under examination is reported; the black area corresponds to the events selected applying the above criteria.

In Fig. 2 symmetrized Dalitz plots [$m^2(\pi^+\pi^-)$ vs $m^2(\pi^+\pi^-)$] for each of the four examined samples are shown. A common feature is evident, i.e., the presence of three bands corresponding to the production of the neutral ρ [$m^2(\pi^+\pi^-)=0.5$ GeV^2], of the $f_2(1270)$ [$m^2(\pi^+\pi^-)=1.6$ GeV^2], and a third band at about $m^2(\pi^+\pi^-)=2.4$ GeV^2, which can be attributed to the production of $f_0(1500)$/$f_2(1565)$. These states can be singled out as well by looking at the $\pi^+\pi^-$ invariant mass projections, reported in Figs. 3(a)–3(d).

Concerning the $\pi^+\pi^+$ invariant mass spectrum, no particular dynamical effect should be observed, but kinematic reflections only. As reported in Figs. 3(e)–3(h), a significant change in the $\pi^+\pi^+$ invariant mass spectra shape is evident as $\overline{n}$ momentum increases, with an enhancement at about 1 GeV; this is probably to be understood as a strong kinematic reflection of $f_2(1270)$.

III. SPIN-PARITY ANALYSIS TECHNIQUES

A. Introduction

The investigation of the nature of $f_0(1500)/f_2(1565)$ had been performed by means of a spin-parity analysis; the properties of this structure and the production of other resonances as well, such as $\rho^0(770)$ and $f_2(1270)$, were studied.

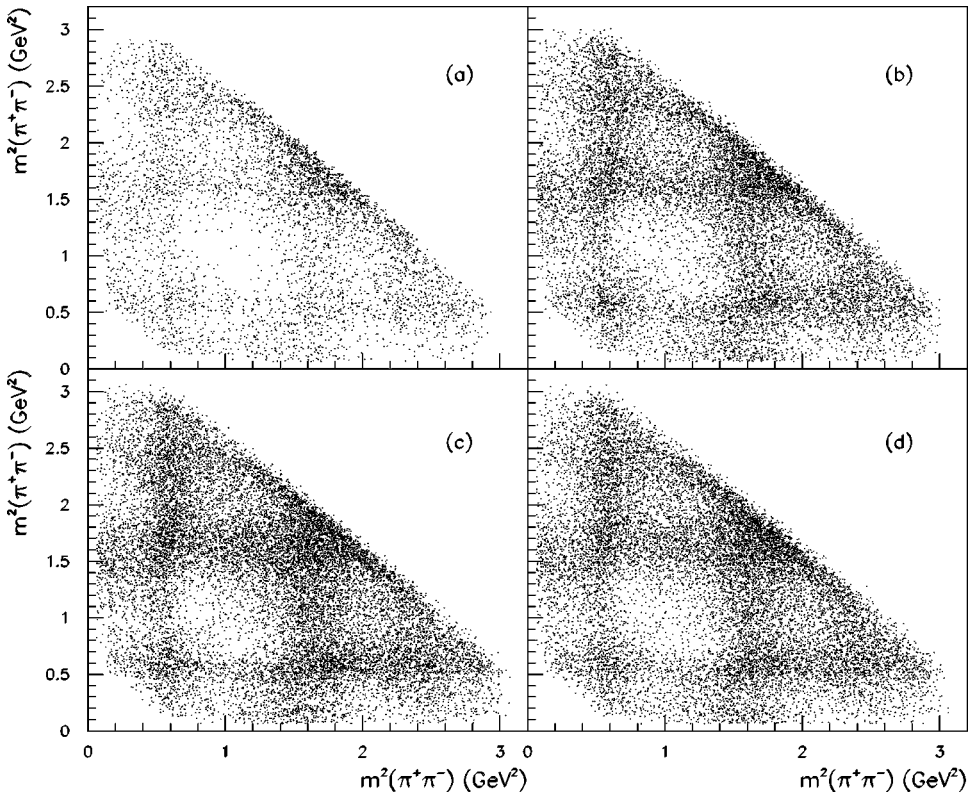

FIG. 2. Symmetrized Dalitz plots: invariant mass squared $(\pi^+_{1,2}\pi^-)$ vs $(\pi^+_{2,1}\pi^-)$. (a) sample 1, $50 \leqslant p_{\overline{n}} \leqslant 200$ MeV/c; (b) sample 2, $200 < p_{\overline{n}} \leqslant 300$ MeV/c; (c) sample 3, $300 < p_{\overline{n}} \leqslant 405$ MeV/c; (d) sample 4, $50 \leqslant p_{\overline{n}} \leqslant 405$ MeV/c.

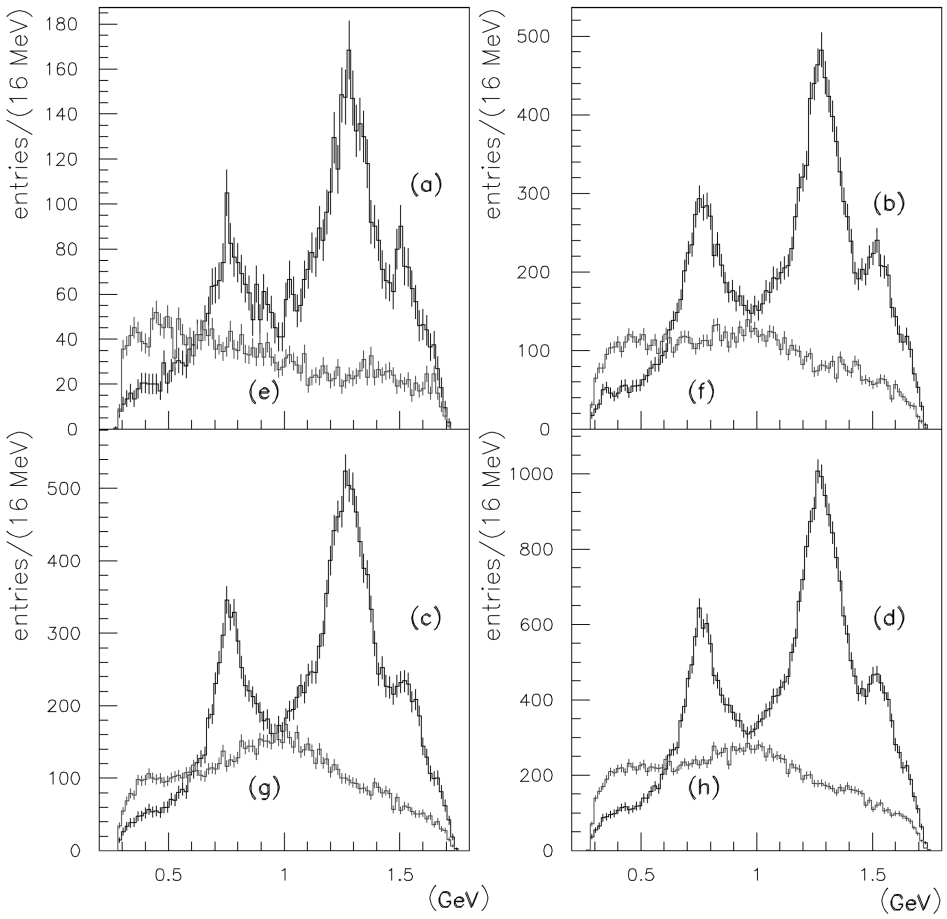

FIG. 3. Dalitz plot projections: Thick black points with errors: $(\pi^+\pi^-)$ invariant mass spectra for (a) sample 1, $50 \leqslant p_{\bar{n}} \leqslant 200$ MeV/c; (b) sample 2, $200 < p_{\bar{n}} \leqslant 300$ MeV/c; (c) sample 3, $300 < p_{\bar{n}} \leqslant 405$ MeV/c; (d) sample 4, $50 \leqslant p_{\bar{n}} \leqslant 405$ MeV/c. Grey points with errors: $(\pi^+\pi^+)$ invariant mass spectra for (e) sample 1, $50 \leqslant p_{\bar{n}} \leqslant 200$ MeV/c; (f) sample 2, $200 < p_{\bar{n}} \leqslant 300$ MeV/c; (g) sample 3, $300 < p_{\bar{n}} \leqslant 405$ MeV/c; (h) sample 4, $50 \leqslant p_{\bar{n}} \leqslant 405$ MeV/c.

The contribution of a scalar $\pi\pi$ S-wave interaction was inserted in the fit as well. Phase shift analyses showed that a large part of this contribution comes from the narrow $f_0(980)$ resonance, coupled to both $\pi\pi$ and $K\bar{K}$, and emerging over a large background which extends from 400 MeV up to about 1.2 GeV. The representation of this contribution is rather problematic and several ways to parametrize it have been proposed in the literature. Some of them are derived from $\pi\pi$ scattering processes in peripheral interactions [22], others from central collisions as well as from other processes. The widely used Au-Morgan-Pennington (AMP) parametrization [23] is, for instance, based on a low energy diffusion data compendium.

A globally unitary treatment of the scalar sector of the amplitude is provided by the K-matrix formalism, used, for example, in Refs. [8,9]. In Ref. [8] the scalar K matrix includes three poles, corresponding to $f_0(980)$, a broad state named as $f_0(1300)$, and $f_0(1500)$. In Ref. [9] a fourth pole was included, corresponding to a wide background resonance [named by the authors as $f_0(1000)$ and classified in last PDG issue as $f_0(400-1200)$]. Lately, a new method for the representation of the scalar amplitude was proposed by Bugg *et al.* [24,25]. In these papers the regions below and above 1.2 GeV are treated separately: the first one by means of a ''partial'' K matrix expressing the interference between $f_0(980)$ and the slowly varying background [the $f_0(400-1200)$], the second one by means of two relativistic Breit-Wigner functions for the description of the resonant states $f_0(1370)$ and $f_0(1500)$.

In the present analysis several tests have been made to single out the best parametrization for the OBELIX data; we will recall later the results of this investigation.

Concerning the vectorial sector, the contribution of a possible radial excitation of the $\rho(770)$ (as a ρ' with unknown mass and width) was inserted in the fits as well. In a recent paper [26] the Crystal Barrel Collaboration suggests that at least two more vector mesons are needed to get a good fit of the channel $\bar{p}d \to \pi^- 2\pi^0 p_s$. The first of them has a mass of 1411 ± 14 MeV and a width of 343 MeV, while the second one peaks at about 1700 MeV. Moreover, a parallel analysis of the channel $\bar{p}p \to \pi^+\pi^-\pi^0$ of OBELIX data (annihilations at rest on hydrogen targets in various density conditions) [4] requires mandatorily at least the first radial excitation at about 1400 MeV. In the present analysis a satisfactory fit is obtained with the lowest mass ρ' only.

B. Global amplitude

The present analysis differs in some aspects from those already described in the literature. First of all $\bar{n}p$ annihilation occurs in flight, and so the square modulus of the total transition amplitude (the ''intensity'') is a sum over the helicity components of the initial states, namely,

$$T_{\rm tot} = \sum_{\lambda_1,\lambda_2} \left| \sum_J H^J_{\lambda_1,\lambda_2} f^J_\lambda \right|^2, \qquad (3.1)$$

where λ_1 and λ_2 are the helicities of $\bar{n}$ and p, $\lambda = \lambda_1 - \lambda_2$, J

is the total angular momentum, $H^J_{\lambda_1,\lambda_2}$ are the helicity couplings, and f^J_λ is the partial wave amplitude projected on the helicity basis.

Each f^J_λ is written as a superposition of partial amplitudes, each related to two-body isobar state i:

$$f^J = \sum_i g^J_i A^J_i \tag{3.2}$$

(we will drop in the following the λ index referring to a definite helicity projection). The g_i's are complex parameters to be determined from a fit of the probability density, normalized to unity, and representing the production strengths of the i two-body state—they can almost be interpreted as branching fractions, in spite of interference effects which will be shown later to be rather weak. The A^J_i partial wave amplitudes for the ith state contains the true dynamics of the problem; they are written as

$$A^J_i = \sum_r Z^{J^{PC}}_{ir}(p,q) F_{ir}(q), \tag{3.3}$$

where $Z^{J^{PC}}$ are known as ''Zemach functions'' [27] and express the spin-angular dependence, while F represents the energy-dependent part, given by proper Breit-Wigner functions in the case of resonances or by different parametrizations for nonresonant interactions, such as the $\pi\pi$ S wave. The index r runs over all the available combinations of two pions forming the ith isobar state. The Zemach covariant tensors [28] are written following the Rarita-Schwinger formulation, by means of the four-momentum vectors of the dipion (q) and of the recoiling pion (p) and depend on the spin J of the resonance and on the relative angular momentum between the resonance products. It was shown that the covariant tensor formalism of Ref. [28] is equivalent to the helicity formalism [20,21] written in the covariant form of Chung [29].

Since the c.m. energy is not too large (<1.92 GeV for $p_{\bar{n}} \lesssim 405$ MeV/c), the partial wave amplitude A^J_i of Eq. (3.3) exhibits in general a centrifugal barrier factor dependence:

$$A^J_i \sim K^{L'} p^L_i q^l_i, \tag{3.4}$$

where L' is the orbital momentum of the initial state and K the nucleon momentum in the $\bar{n}p$ c.m. system; q is as usual the breakup momentum of a spin l dipion and p the momentum of the recoiling pion relative to the dipion, in the c.m. frame of the reaction; finally L is the relative angular momentum between them. The factor $p^L q^l$ expresses the centrifugal barrier factor for primary annihilation into a pion and a resonance and for the subsequent decay of the latter; it is properly taken into account by using the relativistic Zemach tensors. The K dependence may be absorbed into a ''decay form factor'' D, which enters the definition of the dynamical part of the amplitude F_i. In case of resonances it is written as

$$F_{ir} = D^{J,L,l}_{ir} P^{J,L,l}_{ir}. \tag{3.5}$$

Here $P^{J,L,l}_i$ is the relativistic Breit-Wigner propagator, used for the description of resonant dipions with nominal mass m_0, width Γ_0, and decay momentum q_0:

$$P^{J,L,l}(m) = \frac{m_0\Gamma_0}{m_0^2 - m^2 - i m_0 \Gamma(m)}, \tag{3.6}$$

with

$$\Gamma(m) = \Gamma_0 \frac{m_0}{m} \frac{q}{q_0} \frac{W^2_l(q)}{W^2_l(q_0)}; \tag{3.7}$$

the quantities denoted by W are known as Blatt-Weisskopf [30] damping factors:

$$W_0(q) = 1, \tag{3.8}$$

$$W_1(q) = (q\rho)\left(\frac{2}{1+(q\rho)}\right)^{1/2}, \tag{3.9}$$

$$W_2(q) = (q\rho)^2\left(\frac{13}{9+3(q\rho)^2+(q\rho)^4}\right)^{1/2} \tag{3.10}$$

(ρ has been chosen to be 1 fm, a typical value). These quantities appear in the definition of the decay form factors D as well:

$$D^{J,L,l} = K^J W'_J(K) W'_L(p) W'_l(q). \tag{3.11}$$

When using Zemach's method $W'_l(q) = W_l(q)(q\rho)^{-l}$, while in the helicity formalism $W'_l(q) = W_l(q)$. For low $\bar{n}$ momenta the dependence on K is rather flat, and it can be absorbed in the fitting parameters.

The use of an interfering Breit-Wigner formalism had been preferred to a K-matrix one usually adopted in the analyses of annihilations at rest from protonium [8,9]. In fact, the in-flight annihilation is not suitably treated with the K-matrix formalism, since all free parameters (both couplings and partial widths) depend not only on the initial partial wave, but also on the available energy. So the total number of free parameters grows higher, and the convergence of the fits is less easily reached. On the contrary the Breit-Wigner formalism allows a quicker convergence of minimization procedures and the results obtained are simpler to be interpreted and more reliable, due to the reduced number of the free parameters and to their more precise physical meaning.

The conservation of J, P, G, and I (which is fixed) quantum numbers imposes severe restrictions on the number of possible initial partial waves. Because of the low available energy, S- and P-wave initial states only will contribute to the annihilation; the selection rules allow ${}^1S_0(J^P = 0^-)$, ${}^3P_1(J^P = 1^+)$, and ${}^3P_2(J^P = 2^+)$ states. A possible contribution of D waves was shown in a parallel analysis (on five prongs) [31] to have effects of only a few per-

cent, and so it was not inserted in the fit. A similar annihilation frequency from D waves was found in the analysis of the reaction $\overline{n}p \to \pi^+\pi^0$ [32].

The in-flight annihilation mechanism, provided one chooses correctly the working frame (the reaction rest frame with z direction along the $\overline{n}$ momentum vector), involves only some of the initial partial waves available components; using the shorthand S, V, and T notation to indicate $^1S_0$ (scalar), $^3P_1$ (vector), and $^3P_2$ (tensor) waves, $T_{\rm tot}$ may be written as

$$T_{\rm tot} = a^2|S|^2 + b^2|T(0)|^2 + c^2\{|V(+1)|^2 + |V(-1)|^2\} + d^2\{|T(+1)|^2 + |T(-1)|^2\} + 2cd\,\mathrm{Re}\{[V(-1)T^*(-1) - V(+1)T^*(+1)]\exp(i\phi)\}, \quad (3.12)$$

with $a = \sqrt{2}\mathrm{Re}H^S_{++}$, $b = \sqrt{2}\mathrm{Re}H^T_{++}$, $c = \mathrm{Re}H^V_{-+}$, $d = \mathrm{Re}H^T_{-+}$, and $\phi = (\arg H^V_{-+} - \arg H^T_{-+})$. Only orbital angular momenta up to 2 have been considered.

Additional details of the analysis procedure may be found in [33].

C. Treatment of $\pi\pi$ S waves

As already stated in Sec. III A, for the parametrization of the $\pi\pi$ S wave in the mass region under 1.2 GeV, it is not possible to use a simple propagator and decay factor, but it is necessary to adopt a complex amplitude which could describe the two-body elastic scattering $\pi\pi \to \pi\pi$, as well as, at least, the inelastic scattering $\pi\pi \to K\overline{K}$, due to the opening of $K\overline{K}$ threshold.

Strictly speaking, none of the $\pi\pi$ S waves available in the literature really fits the production environment of the $\overline{n}p \to 2\pi + \pi^-$ annihilation. Therefore several tests have been performed to check the consistency of various kinds of parametrizations. The AMP parametrization [23], the one used by Gaspero in Ref. [34], and that proposed by Bugg *et al.* [24] and used in [25], have been chosen to this end. The parametrization by Gaspero [34] reproduces phenomenologically, by means of a polynomial interpolation, some sets of phase shift data collected by various experiments. The production fractions of initial partial waves and of resonant intermediate states obtained both with Gaspero's and with AMP parametrization are, within errors, equivalent; full details of these results are reported in [33].

The best results are anyway obtained in our analysis by using the parametrization by Bugg *et al.* [24], described in Sec. III A. In this case, the elements of the two-pole K matrix used for the description of the ''low mass'' scalar sector, which will be globally referred to as σ in the following, are weighted by means of complex production coefficients, directly taken from Ref. [24]. The energy-dependent part of the scalar amplitude, to be directly inserted in Eq. (3.3), is written as

$$F_\sigma = \frac{(\Lambda_1 + \Lambda_2 s)\hat{K}_{11} + \Lambda_3\hat{K}_{12}}{1 - \rho_1\rho_2\hat{D} - i(\rho_1\hat{K}_{11} + \rho_2\hat{K}_{22})}, \quad (3.13)$$

where Λ_i are the cited complex production parameters, ρ_i are usual elements of the two-body phase-space matrix; $\hat{D}$ is the K-matrix determinant, while $\sqrt{s}$ is, as usual, the c.m. available energy. Since in our analysis the Λ_i production parameters are fixed, we are not able to separate the different contributions of $f_0(980)$ and of $f_0(400-1200)$ to the global σ state.

The two ''low mass'' scalar poles resemble in a way the two low mass ones embedded in the AMP parametrization. Above 1.2 GeV the AMP parametrization includes an additional S-matrix pole also, at about 1400 MeV. In the approach of Bugg *et al.* [24] this contribution is inserted as an interfering relativistic Breit-Wigner function, with mass and width to be adjusted by the fit, and represents what is generally understood to be the $f_0(1370)$ state, which several analyses claim to be about 350 MeV broad [3].

In the following we will describe the results obtained applying this parametrization to our data.

D. Fits quality estimators

Because of the event-by-event dependence on energy, the correct function to be minimized is the negative logarithm of the global likelihood probability density:

$$\mathcal{L} = \prod_{i=1}^{N} \frac{\mu_i}{\int \mu\, d\Omega}, \quad (3.14)$$

where μ_i is the event-by-event intensity, properly normalized by means of a large number of pure phase-space Monte Carlo events, and μ is the total probability density evaluated by using the Monte Carlo-generated events. In this way all elementary amplitudes take quite naturally into account the apparatus efficiency and acceptance.

With three charged pions the acceptance of the OBELIX apparatus is nearly flat (within 3%). In this case it is possible to perform fits with reasonably small Monte Carlo samples without losing statistical significance for the larger contribution by systematic errors. It was chosen to use Monte Carlo samples about 3 times as wealthy as the corresponding experimental ones.

The quality of fits can be gathered by studying, in addition to the trend of the likelihood value, the χ^2 evaluated on the theoretical symmetrized Dalitz plot, defined as [2]

$$\chi^2_D = \sum_{i,j}^{\rm cells} \frac{(n_{ij} - t_{ij})^2}{\sigma^2_{\rm expt} + \sigma^2_{\rm th}}, \quad (3.15)$$

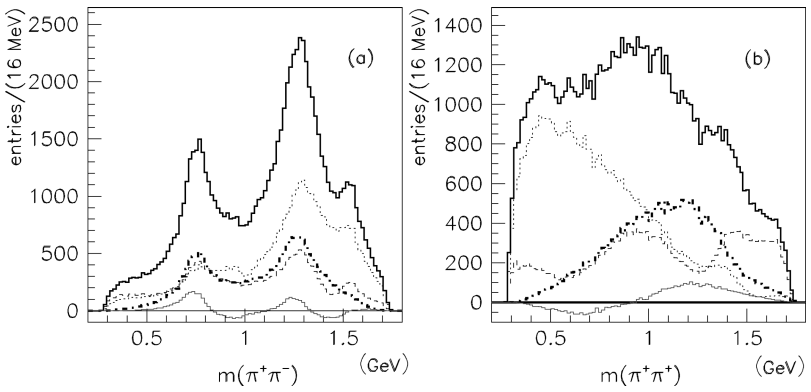

FIG. 4. Contribution of each partial wave to the global spectra (Monte Carlo events modeled by the fit, $\sim 50 \leqslant p_{\bar{n}} \leqslant 405$ MeV/c sample), for (a) the $(\pi^+\pi^-)$ invariant mass distribution and (b) for the $(\pi^+\pi^+)$ one. The partial spectra correspond, respectively, to total (solid lines), $^3P_1$ contribution (dotted line), $^3P_2$ contribution (thick dashed line), $^1S_0$ contribution (dashed line), interference contribution (solid thin grey line).

where n_{ij} and t_{ij} (σ_{expt} and σ_{th}) are the global contents (errors) of the ijth cell of experimental and theoretical Dalitz plots. In the evaluation of symmetrized Dalitz plot χ^2 the errors on the cell contents are given by $\sigma^2_{\text{expt}} = n_{ij}/2$ (due to the fact that each event has two entries: n is the effective number of physical events belonging to ijth cell). For the theoretical plot, on the contrary, for each of the cells we have

$$\sigma^2_{\text{th}} = \sum^{\text{events}} w^2_{ij}/2 = t^2_{ij}/2p_{ij}, \tag{3.16}$$

where w_{ij} is the weight (squared amplitude) of each of the phase space Monte Carlo events belonging to the ijth cell, whose number per cell is p_{ij}. t_{ij} is now obtained by the simple sum of w_{ij} weights for all of the Monte Carlo event belonging to the ijth cell.

The theoretical Dalitz plot and the experimental one are normalized to the same number of entries, and for the χ^2 evaluation only the cells with more than five events were taken into account. Since the Monte Carlo data samples are larger by a factor of at least 2 than the experimental ones, each Monte Carlo–modeled spectrum is affected by a statistical error which amounts to about the 60–70 % of that actually affecting the experimental data distributions.

E. Production fractions

The production rates of each initial partial wave are calculated as

$$f_{J^{PC}} = \frac{\sum_{\lambda} w^{\lambda}_{J^{PC}} |H^{\lambda}_{J^{PC}}|^2}{\sum_{J} \sum_{\lambda} w^{\lambda}_{J^{PC}} |H^{\lambda}_{J^{PC}}|^2}, \tag{3.17}$$

where the helicity amplitudes H are inferred from the fit [the a, b, c, and d coefficients of Eq. (3.12)] and the $w^{\lambda}_{J^{PC}}$'s are statistical spin weights of each amplitude, obtained by integration over the full available spectrum.

Each $|H^{\lambda}_{J^{PC}}|^2$ gives the probability of the occurrence of the λ component of a given J^{PC} initial state only, and this has to be taken into account when constructing the total probability density. The spin weights have the same meaning of the partial wave amplitude in Eq. (3.12), after integration over the spectrum.

The contribution of the interference term, coming from the combination of $^3P_1$ and $^3P_2$ $\lambda = \pm 1$ components, is always less than 3%; this can be inferred from Fig. 4, which shows the contribution of each partial wave—and of the interference term as well—to the total amplitude, for data in the ~ 50–400 MeV/c full momentum range. In Fig. 4, the lower line (solid gray) corresponds to the interference contribution.

In a similar way, the branching fractions for all isobars have been evaluated as in [2]:

$$\text{BF}_i = \sum_J \frac{x_i^2}{\sum_l x_l^2} f_{J^{PC}}, \tag{3.18}$$

where the x_i values, which express the production weights for the i-type isobar and depend on the J^{PC} quantum numbers of the state, are obtained from the minimization procedure. Using Eq. (3.18) the interference effects between resonances are, again, necessarily neglected; provided they are not too heavy, the ''branching fraction'' values represent a reliable suggestion of the strength of the production of a single state.

IV. RESULTS FROM THE FITS

A. Strategy

The main difference from the previous analyses is that f_0/f_2 masses and widths are left free in the fits, and so for each of them minimization errors can be quoted. On the contrary, the ρ^0 and $f_2(1270)$ masses have been fixed to the values quoted by PDG [3]; a fit on the shape on $\pi^+\pi^-$ invariant mass spectrum with noninterfering Breit-Wigner functions shows a quite good agreement of the OBELIX data to them. The mass and width of the other unknown states, namely, the $f_0(1370)$ and the $\rho'(1450)$, were searched for afterwards, after having settled those of the structures in the 1500 MeV region.

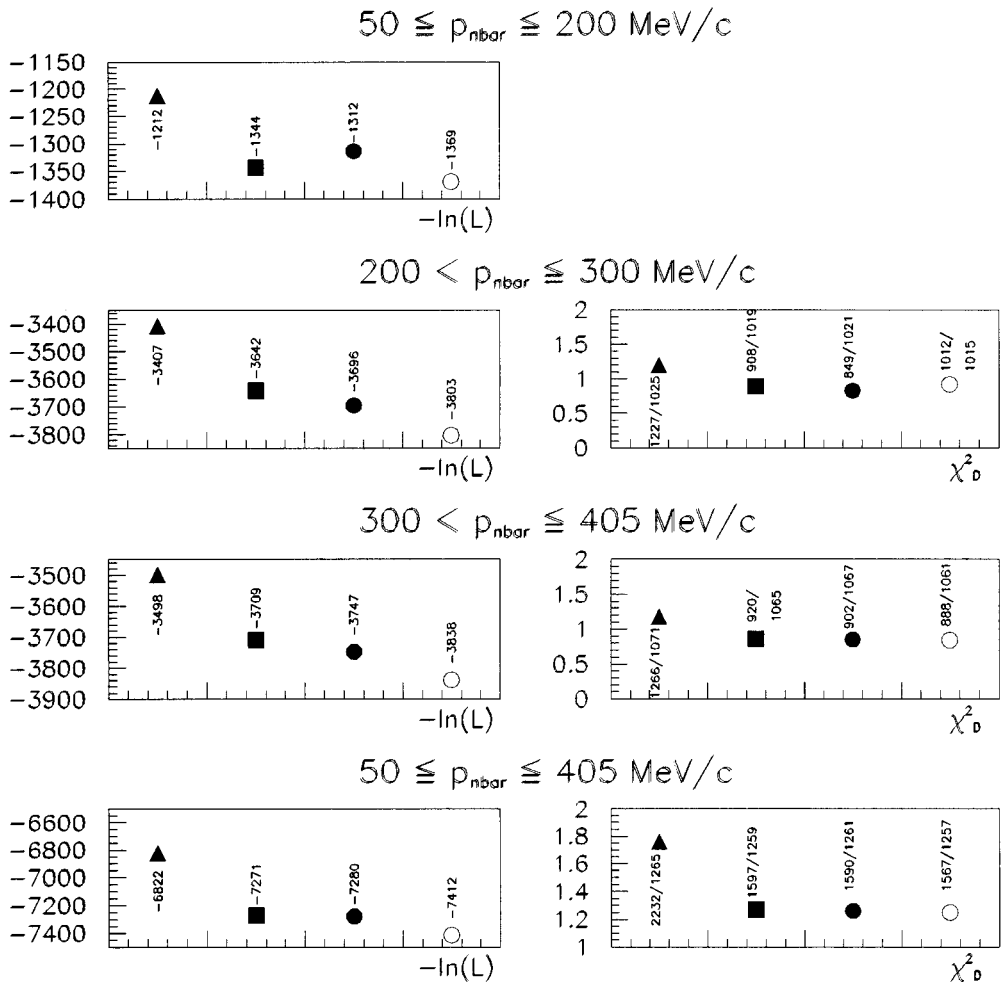

FIG. 5. Trend of quality of fit estimators ($-\ln\mathcal{L}$ and χ^2 calculated on the Dalitz plot), for the best fit obtained in all of the four data samples under examination. The markers correspond to the different hypotheses: (1) black triangle, no resonance in the 1500 MeV region; (2) black squares, tensorial signal only; (3) black circle, scalar signal only; (4) open circle, both scalar and tensorial resonances. The χ^2_D for the less wealthy data sample ($\sim 50 \leqslant p_{\bar{n}} \leqslant 200$ MeV/c) is not reported since the available statistics is too scarce to have enough populated cells (five events for a cell at least) for a reliable calculation.

Four independent analyses were carried over for data belonging to the cited samples. As a general result, the fits with the double contribution by either $f_0(1500)$ and $f_2(1565)$ give better results both for $\mathcal{L}$ values, and for χ^2 evaluated on Dalitz plots; the fits with the scalar contribution only always show a better likelihood value in comparison to a single tensorial signal. This result is clearly shown in Fig. 5, where for the values of $\ln\mathcal{L}$ and χ^2_D are separately reported for each data sample under examination, with reference to fits performed in the four different hypotheses (a) (black triangles) no resonance in the region at about 1500 MeV, (b) (black squares) tensorial signal only, (c) (black circles) scalar signal only, and (d) (open circles) both scalar and tensorial signals.

All the results relative to the behavior in the 1500 MeV region are independent of the method chosen to parametrize $\pi\pi$ S-wave contribution.

B. Final results

All the results which will be quoted here have been obtained by convergent and stable fits. They all refer to a ''minimum environment'' which had been found in a thorough independent way for each data sample.

Quoting as systematic error the maximum spread of the masses and widths values obtained in the best fit solutions and as statistical ones the maximum of the minimization errors delivered by MINUIT [35] in all of the performed fits, the average values (over the whole $\bar{n}$ momentum spectrum) for f_0 and f_2 masses and widths are

$$m(f_0(1500)) = 1522 \pm 5_{\text{stat}} \pm 25_{\text{syst}} \quad \text{MeV},$$

$$\Gamma(f_0(1500)) = 108 \pm 8_{\text{stat}} \pm 32_{\text{syst}} \quad \text{MeV},$$

$$m(f_2(1565)) = 1575 \pm 15_{\text{stat}} \pm 10_{\text{syst}} \quad \text{MeV},$$

$$\Gamma(f_2(1565)) = 119 \pm 18_{\text{stat}} \pm 16_{\text{syst}} \quad \text{MeV}.$$

After having set these values it was checked whether the insertion of new states not directly emerging from the Dalitz

TABLE II. Comparison between quality of fit estimators in different best fits performed on the sample with the greatest available statistics (35 118 events), by means of scalar amplitude parametrized as in Ref. [24,25] [(1c) and following], and in the case of AMP [(1a)] [23] and Gaspero's version [(1b)] [34].

	$\ln\mathcal{L}$	χ^2_D
(1a) σ AMP	−7412	2098/1257
(1b) σ Gaspero [34]	− 7425	1906/1257
(1c) σ [24,25]	−7467	1939/1251
(2) σ + $f_0(1370)$	−7494	1826/1232
(3) σ + $f_0(1370)+\rho'(1450)$	−7741	1567/1239

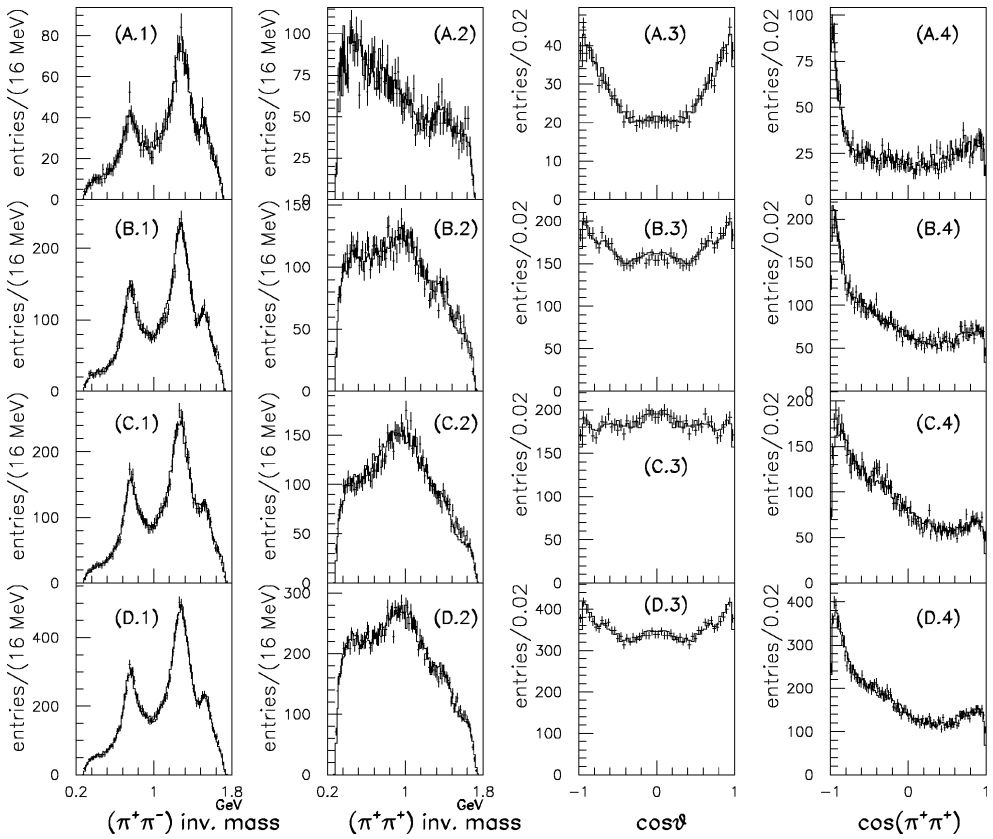

FIG. 6. Results from fit: the solid black line represents the fit, and the points with errors are the experimental data. On vertical rows the plots refer to the different data samples: type (A) $\sim 50 \leqslant p_{\bar{n}} \leqslant 200$ MeV/c, type (B) $200 < p_{\bar{n}} \leqslant 300$ MeV/c, type (C) $300 < p_{\bar{n}} \leqslant 405$ MeV/c, and type (D) $50 \leqslant p_{\bar{n}} \leqslant 405$ MeV/c. The following spectra are presented on horizontal lines: type (1), $(\pi^+\pi^-)$ invariant mass; type (2), $(\pi^+\pi^+)$ invariant mass; type (3), angle θ between the recoiling π^+ (in the dipion c.m.) and the dipion line of flight in reaction rest frame; type (4), angle between the two π^+'s in the laboratory frame.

plots, namely, $f_0(1370)$ and $\rho'(1450)$, could produce any significant change in the quality of the fits. The effect of the introduction of these two states may be better evaluated by studying the trend of the quality estimators in the fits performed on the most wealthy data sample. In Table II the values of $-\ln\mathcal{L}$ and χ^2_D obtained in the three different hypotheses: (1) σ contribution only, (2) σ and $f_0(1370)$ contributions, and (3) σ, $f_0(1370)$, and $\rho'(1450)$ contributions are reported. Concerning the first hypothesis, lines (1a), (1b), and (1c) report, respectively, the values of the estimators obtained in a fit to the same data sample by using for the σ state the AMP parametrization, Gaspero's one, and the one suggested by Bugg *et al.*, for comparison purposes.

The greater flexibility of the amplitude suggested by Bugg *et al.* immediately delivers better values for all of the estimators even in the simpler hypothesis (1) [presence of scalar interaction below 1.2 GeV only, without $f_0(1370)$ contribution]; a greater improvement is gained with the introduction of the ρ' signal. The best fits occurs for the following values for $f_0(1370)$ and $\rho'(1450)$ masses and widths:

$$m(f_0(1370)) = 1280 \pm 55_{\text{stat}} \quad \text{MeV},$$

$$\Gamma(f_0(1370)) = 323 \pm 13_{\text{stat}} \quad \text{MeV},$$

$$m(\rho'(1450)) = 1348 \pm 33_{\text{stat}} \quad \text{MeV},$$

$$\Gamma(\rho'(1450)) = 275 \pm 10_{\text{stat}} \quad \text{MeV},$$

where the errors are statistical only and express the maximum minimization error obtained in several fits.

The introduction of these states has no effect on the production fractions of the states located in the 1500 MeV region; the superposition of the σ state and of the $f_0(1370)$ contribution is about equivalent (within errors) to the global $\pi\pi$ S-wave contribution obtained by means of AMP parametrization. In spite of the differences in the parametrizations, the mass and width values keep on being in good agreement to the mean values reported above; this shows the stability of

TABLE III. Initial partial waves fractions in percent for the different ranges of $\bar{n}$ momentum under examination. The last row represents the values obtained for the χ^2 on Dalitz plots.

	$\sim$50–200 MeV/c	200–300 MeV/c	300–405 MeV/c
$^1S_0$	$26.0 \pm 0.3 \pm 3.2$	$24.9 \pm 0.1 \pm 3.2$	$22.4 \pm 0.1 \pm 2.1$
$^3P_1$	$55.7 \pm 0.6 \pm 4.4$	$49.3 \pm 0.2 \pm 2.8$	$44.8 \pm 0.2 \pm 3.2$
$^3P_2$	$15.88 \pm 0.08 \pm 4.49$	$23.3 \pm 0.1 \pm 2.5$	$31.4 \pm 0.1 \pm 2.3$
Interference	$2.50 \pm 0.06 \pm 0.05$	$2.44 \pm 0.03 \pm 1.71$	$1.47 \pm 0.02 \pm 0.90$
χ^2_D	0.93	1.11	1.03

TABLE IV. Isobar branching fractions in percent for different ranges of $\bar{n}$ momentum. σ parametrized following Refs. [24,25].

	~50–200 MeV/c	200–300 MeV/c	300–405 MeV/c
σ	$28.9\pm0.1\pm12.2$	$17.60\pm0.06\pm6.53$	$11.54\pm0.04\pm10.60$
$\rho^0(770)$	$6.24\pm0.04\pm3.05$	$18.21\pm0.04\pm3.20$	$14.05\pm0.04\pm4.47$
$f_2(1270)$	$10.12\pm0.06\pm4.22$	$25.06\pm0.05\pm10.00$	$36.6\pm0.1\pm8.8$
$f_0(1370)$	$32.08\pm0.10\pm7.48$	$6.55\pm0.02\pm12.59$	$9.60\pm0.03\pm14.06$
$\rho'(1450)$	$9.02\pm0.06\pm1.8$	$15.72\pm0.04\pm3.72$	$10.51\pm0.03\pm5.62$
$f_0(1500)$	$10.17\pm0.06\pm1.59$	$10.21\pm0.03\pm1.31$	$9.69\pm0.03\pm1.88$
$f_2(1565)$	$3.48\pm0.03\pm1.29$	$6.63\pm0.02\pm2.94$	$7.95\pm0.03\pm1.01$

the achieved solution and its independence of the way the background $\pi\pi$ interaction is represented.

Concerning the other resonant state production fractions obtained by means of AMP and/or Gaspero's parametrizations, they are somewhat different from those obtained with the one of Bugg *et al.*; this is seemingly due to the absence of $f_0(1370)$ contribution, which in both AMP and Gaspero's treatments was not inserted in order to avoid possible double counting. This difference is evident especially in the production of $f_2(1270)$ mesons; moreover, the production rates are altered by the presence of a ρ' state. The effect of this ρ' signal is to lower the $f_2(1270)$ production rate, since the two states are overlapping. Full details of the results obtained by using AMP and Gaspero's parametrizations are reported in Ref. [36].

Some typical distributions, with the results of the fits obtained using the parametrization of the Bugg *et al.* superimposed, are shown in Fig. 6 for the four data samples under examination.

In Table III the production fractions of each partial wave, normalized to 100%, are reported, as a function of the $\bar{n}$ momentum. The first quoted errors are statistical and are obtained by simple Gaussian propagation on the values delivered by MINUIT; the second ones are systematic and take into account the spread of the parameter values delivered in several acceptable fits. Table IV reports the partial branching fractions of each resonant state, evaluated by means of Eq. (3.18). All results are reported for the three data samples 1, 2, and 3.

From Tables III and IV the following general trends may be inferred, as the incoming $\bar{n}$ momentum increases: a decrease in S-wave production and a slight increase of P wave production, resulting from a steep increase of the $^3P_2$ component as well as a softer decrease of $^3P_1$ one; concerning the branching fractions a decreasing contribution of the $\pi\pi$ S wave below 1.2 GeV (σ); an almost constant contribution from $f_0(1500)$; a strongly increasing production of $f_2(1270)$; an increasing production fraction of $f_2(1565)$; the trends for the production of both vectorial mesons, namely, $\rho^0(770)$ and ρ', are somewhat similar, not showing a monotonical trend but rather a maximum in the range 200–300 MeV/c; a somewhat decreasing production of $f_0(1370)$, although affected by rather large errors; the production of the scalar component $f_0(1500)$ is always dominant over $f_2(1565)$; the errors are still too large to assert any specific trend, but the already mentioned increase of $f_2(1565)$ production with the increase of $\bar{n}$ momentum.

V. CONCLUSIONS

The present analysis, performed on the total sample of $\bar{n}p\to\pi^+\pi^+\pi^-$ annihilation data, collected by the OBELIX experiment, led to obtain the masses and widths values for both $f_0(1500)$ and $f_2(1565)$. These values agree well, within errors, to what previously found by other experiments and reported by PDG [3]. The $f_0(1500)$ features are, in addition, in full agreement to what is obtained by the OBELIX experiment in a parallel analysis on the $\bar{p}p\to\pi^+\pi^-\pi^0$ channel [4]. In this channel, the interference mechanism between charged ρ's may be at the origin of the slight difference concerning the $f_2(1565)$ mass.

In conclusion, by exploiting a good deal of high quality data, we confirm the presence of a scalar resonance in the 1500 MeV mass region, as well as a weaker tensorial structure, of similar mass and width. Their overall contribution amounts to about 15% of the whole spectrum, a value in good agreement with a preliminary evaluation, based on not interfering Breit-Wigner integration and performed on a limited statistics set of data [16].

The production fractions of both the states, as well as their masses and widths, remain stable within statistical and systematic errors even when the fits are performed with different starting conditions, and with different kinds of parametrizations of the $\pi\pi$ nonresonating S wave, in the region below under 1.2 GeV.

ACKNOWLEDGMENTS

We gratefully acknowledge the LEAR operating staff for the excellent $\bar{p}$ beam quality and the intensity that could be successfully provided during the dedicated runs. We are particularly indebted to G. Bochaton, V. Mazzone, G. Novellini, and V. Sergo for their invaluable contribution in designing, constructing, and operating the cryogenic targets used in the experiment. F. Impavido and A. Pia provided clever assistance in the construction and setting up of the mechanical elements of the antineutron beam.

[1] S. Devons *et al.*, Phys. Lett. **47B**, 271 (1973); P. Anninos *et al.*, Phys. Rev. Lett. **20**, 402 (1968).
[2] Asterix Collaboration, B. May *et al.*, Z. Phys. C **46**, 191 (1990); **46**, 203 (1990).
[3] Particle Data Group, R. M. Barnett *et al.*, Phys. Rev. D **54**, 1 (1996).
[4] OBELIX Collaboration, A. Bertin *et al.*, Phys. Lett. B **408**, 476 (1997).
[5] Crystal Barrel Collaboration, E. Aker *et al.*, Phys. Lett. B **260**, 249 (1991).
[6] Crystal Barrel Collaboration, V. V. Anisovich *et al.*, Phys. Lett. B **323**, 233 (1994).
[7] Crystal Barrel Collaboration, C. Amsler *et al.*, Phys. Lett. B **291**, 347 (1992).
[8] Crystal Barrel Collaboration, C. Amsler *et al.*, Phys. Lett. B **342**, 433 (1995).
[9] Crystal Barrel Collaboration, C. Amsler *et al.*, Phys. Lett. B **355**, 425 (1995).
[10] V. V. Anisovich *et al.*, Phys. Rev. D **50**, 1972 (1994).
[11] S. U. Chung *et al.*, Ann. Phys. (Leipzig) **4**, 404 (1995); I. J. R. Aitchinson, Nucl. Phys. **A189**, 417 (1972).
[12] OBELIX Collaboration, A. Adamo *et al.*, Nucl. Phys. **A558**, 13c (1993).
[13] OBELIX Collaboration, V. G. Ableev *et al.*, in *Proceedings Third Biennal Conference on Low-Energy Antiproton Physics*, Bled, Slovenia, 1994, edited by G. Kernel, P. Krizan, and M. Mikuz (World Scientific, Singapore, 1995), p. 75.
[14] OBELIX Collaboration, A. Bertin *et al.*, Phys. At. Nucl. **59**, 1378 (1996).
[15] T. E. Kalogeropoulos *et al.*, Phys. Rev. D **24**, 1759 (1981).
[16] OBELIX Collaboration, A. Adamo *et al.*, Phys. Lett. B **287**, 368 (1992).
[17] OBELIX Collaboration, A. Adamo *et al.*, Sov. J. Nucl. Phys. **55**, 1732 (1992).
[18] G. C. Bonazzola *et al.*, Nucl. Instrum. Methods Phys. Res. A **356**, 270 (1995).
[19] M. Agnello *et al.*, Nucl. Instrum. Methods Phys. Res. A **399**, 11 (1997).
[20] C. Amsler and J. Bizot, Comput. Phys. Commun. **30**, 21 (1983).
[21] S.U. Chung, ''Spin Formalisms,'' CERN Yellow Report No. CERN 71-8, 1971.
[22] B. Hyams *et al.*, Nucl. Phys. **B100**, 205 (1975).
[23] K. L. Au, D. Morgan, and M. R. Pennington, Phys. Rev. D **35**, 1633 (1987).
[24] D. V. Bugg *et al.*, Nucl. Phys. **B471**, 59 (1996).
[25] A. Abele *et al.*, Nucl. Phys. **A609**, 562 (1996).
[26] Crystal Barrel Collaboration, A. Abele *et al.*, Phys. Lett. B **391**, 191 (1997).
[27] C. Zemach, Phys. Rev. **140**, B97 (1965); **140**, B109 (1965).
[28] V. Filippini, A. Fontana, and A. Rotondi, Phys. Rev. D **51**, 2247 (1995).
[29] S. U. Chung, Phys. Rev. D **48**, 1225 (1993).
[30] F. von Hippel and C. Quigg, Phys. Rev. D **5**, 624 (1972); Crystal Barrel Collaboration, C. Amsler *et al.*, Phys. Lett. B **311**, 362 (1993).
[31] OBELIX Collaboration, V. G. Ableev *et al.*, in *Proceedings HADRON 95 Conference*, Manchester, England, 1995; edited by M. C. Birse, G. D. Lafferty, and J. A. McGovern (unpublished), p. 337.
[32] B. Giacobbe, in *Leap 96, Proceedings of the Conference*, Dinkelsbühl, Germany, 1996, edited by H. Koch *et al.* [Nucl. Phys. (Proc. Suppl.) **56A**, 227 (1997)].
[33] A. Filippi, Ph.D. thesis, Università degli Studi di Pavia, 1996.
[34] M. Gaspero, Sov. J. Nucl. Phys. **55**, 795 (1992); M. Gaspero, Nucl. Phys. **A562**, 407 (1993).
[35] F. James and M. Roos, computer code MINUIT, CERN DD Long Writeup, D506, CERN, 1987.
[36] A. Filippi, in *LEAP 96* [32], p. 160.